






Branched droplet clusters and the Kramers theorem

Mark Frenkel ¹, Alexander A. Fedorets ², Dmitry V. Shcherbakov,² Leonid A. Dombrovsky ^{1,2,3},
Michael Nosonovsky ^{2,4,*} and Edward Bormashenko ¹

¹*Department of Chemical Engineering, Engineering Faculty, Ariel University, Ariel 407000*

²*X-BIO Institute, University of Tyumen, 6 Volodarskogo St., Tyumen 625003, Russia*

³*Joint Institute for High Temperatures, 17A Krasnokazarmennaya St., Moscow 111116, Russia*

⁴*Mechanical Engineering, University of Wisconsin—Milwaukee, 3200 North Cramer St., Milwaukee, Wisconsin 53211, USA*



(Received 12 January 2022; accepted 17 April 2022; published 16 May 2022)

Scaling laws inherent for polymer molecules are checked for the linear and branched chains constituting two-dimensional (2D) levitating microdroplet clusters condensed above the locally heated layer of water. We demonstrate that the dimensionless averaged end-to-end distance of the droplet chain \bar{r} normalized by the averaged distance between centers of the adjacent droplets \bar{l} scales as $\bar{r}/\bar{l} \sim n^{0.76}$, where n is the number of links in the chain, which is close to the power exponent $3/4$, predicted for 2D polymer chains with excluded volume in the dilution limit. The values of the dimensionless Kuhn length $\bar{b} \cong 2.12 \pm 0.015$ and of the averaged absolute value of the bond angle of the droplet chains $|\bar{\theta}| = 22.0 \pm 0.5^\circ$ are determined. Using these values we demonstrate that the predictions of the Kramers theorem for the gyration radius of branched polymers are valid also for the branched droplets' chains. We discuss physical interactions that explain both the high value of the power exponent and the applicability of the Kramers theorem including the effects of the excluded volume, surrounding droplet monomers, and the prohibition of extreme values of the bond angle.

DOI: [10.1103/PhysRevE.105.055104](https://doi.org/10.1103/PhysRevE.105.055104)

I. INTRODUCTION

Branched physical systems are ubiquitous in physics [1,2], chemistry [3], biology [4], and engineering [5,6]. It seems that the physics of branched systems was first addressed by Leonardo da Vinci, who observed in his notebooks that “all the branches of a tree at every stage of its height when put together are equal in thickness to the trunk” [7,8]. In our study, we explore branched chainlike structures built of microscale water droplets.

Branched droplet systems have been already addressed by the researchers [9–12]. In particular, branched chainlike droplet structures arising from the phase separation in the mixtures of a polymer and a nematic liquid crystal were reported [10]. The formation of branched droplet structures was observed under the confined Ouzo effect (i.e., spontaneous emulsification) [13]. We reported the branched chainlike structures built of droplets in the so-called droplet clusters, a novel phenomenon discovered in 2004 by Fedorets, who demonstrated that a self-assembled monolayer of microdroplets emerges over a locally heated (typically, at 60–95 °C) surface of the water [14–17]. Growing condensing droplets with a typical diameter of 10–200 μm are supported by a vapor-air rising flow over the heated spot. The droplets levitate at an equilibrium height, where their weight is equilibrated by the vertical component of the drag force. The height of levitation and the distance between the droplets are of the same order as their diameters [14–17]. A diversity of approaches to

the explanation of the origin and properties of droplet clusters were suggested [18–20]. The mechanism of formation of the levitating cluster is complicated and involves aerodynamic and electrostatic interactions [21–24]. In spite of the much experimental and theoretical effort spent on the study of the droplet cluster, the precise mechanism of its formation and self-ordering remains obscure.

Levitating droplet clusters can be viewed as an example of self-assembled colloidal systems, and broadly speaking, of diffusion-limited aggregation systems, which often have a treelike or branched structure. We will demonstrate in the present paper that the ideas learned from the polymer science may be effectively applied for the phenomenological analysis of the linear and branched chains in the levitating droplet clusters.

II. EXPERIMENTAL METHODS

The experimental procedure described in our previous publications was used in the present study [16]. The droplet cluster was self-assembled over the locally heated surface of a thin layer of distilled water. The thickness of the water layer ($400 \pm 2 \mu\text{m}$) was controlled using the confocal chromatic sensor IFC2451 made by the company Micro-Epsilon (USA). The cuvette temperature was equal to $10 \pm 0.5^\circ\text{C}$. The water layer was placed on a flat sital substrate of 400- μm thickness. The lower surface of this substrate was blackened to absorb the radiation at the $808 \pm 5 \text{ nm}$ wavelength emitted by the laser BrixX 808-800HP (Omicron Laserage, Germany). The diameter of the laser beam at the substrate surface was equal to 1 mm. The laser power was controlled by a PM200 device

*Corresponding author: nosonovs@uwm.edu

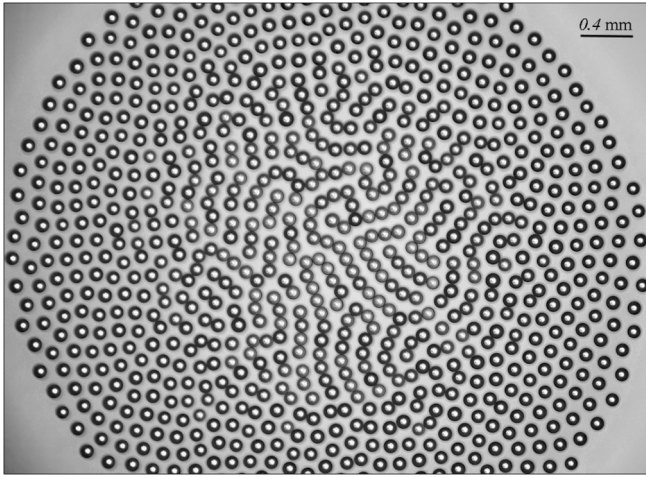


FIG. 1. Branched droplet chains within the droplet cluster.

equipped with an S401c sensor (Thorlabs, USA). Video images of the cluster were taken using a Zeiss AXIO Zoom.V16 stereomicroscope (Germany) and high-speed (1000 frames per second) PCO.EDGE 5.5C video camera (Germany) with a spatial resolution of $0.6 \mu\text{m}$. The region of the droplet cluster is schematically presented in Fig. 1. Images were treated with the laboratory made software, based on the OpenCV image processing library. See Supplemental Material 1 [25] for the Video showing the dynamic behavior of the chains in the cluster.

III. RESULTS AND DISCUSSION

A. The scaling laws and the Khun length inherent for linear droplet chains

We have already reported the formation of “linear”, “chain-like” and “branched” polymerlike configurations of droplet clusters. In the “chain state” (chain configuration), droplets almost touch each other, however, do not coalesce [17]. The transition from the regular (hexagonal) arrangement of the droplet cluster to the chain cluster is abrupt, and it is observed at a certain critical ratio of droplet size and packing density. The lifetime of the chain cluster is about 20–30 s on average, and the transition is reversible [17]. The first approximation of the droplet chain by the free-joint model of the polymer (oligomer) chain predicts the random walk dependency of the average end-to-end distance, namely $\langle r^2 \rangle = Cnl^2$, where C is called Flory’s characteristic ratio, n is the number of links in the chain ($n = m - 1$, where m is the number of monomers (droplets) and l is the chemical bond length). Obviously, when we study the polymerlike chain built from the identical droplets with the diameter D it is plausible to assume the scaling dependence: $\langle r^2 \rangle = CnD^2$.

Consider the long droplet chains, in which droplets interact one with another, seen as polymer chains, on which monomers interact. In this case the Flory approach predicts the following scaling law, applicable for real polymer chains:

$$\bar{r} \approx bN^\nu, \quad (1)$$

where \bar{r} is the averaged end-to-end distance of the chain and b is the so-called Kuhn segment length of the polymer chain,

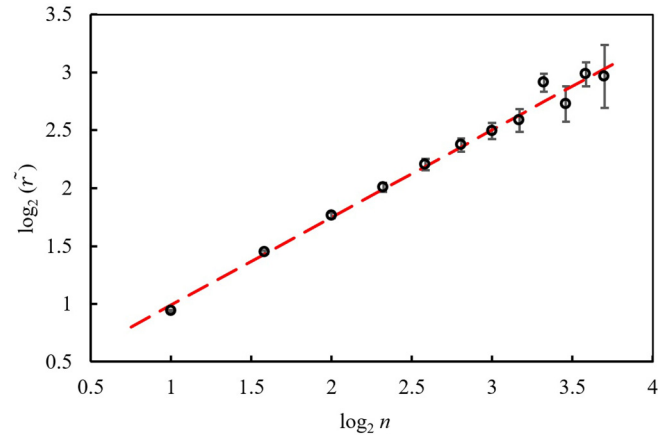


FIG. 2. The double-log plot of the nondimensional end-to-end distance in nonbranched droplet chains vs the number of links in the chain. The linear fitting supplies the scaling law $\bar{r} \sim n^{0.76}$ (the squared standard deviation $R^2 = 0.9878$). The standard deviation is growing with the length of the chain because the number of small chains increases. The results summarize the analysis of 823 droplet chains.

N is the number of freely joined effective bonds of length b , and ν is a power exponent. For 3D ideal chains built of noninteracting monomers $\nu = \frac{1}{2}$ [26]. The Flory theory of a random 3D polymer chain with excluded volume predicts the value of the power exponent of $\nu = 3/5$ (or $\nu = 0.588$ based on more elaborated renormalization arguments) [27]. It should be emphasized that for two-dimensional (2D) chains with excluded volume the scaling theory predicts $\nu = \frac{3}{4}$ and this law is universal for the models considering the excluded volumelike repulsion of monomers [28]. Two additional factors may affect the value of the exponent. First, the presence of many other chains surrounding the molecule affects its shape and makes it less compact than in the case of a single molecule, and this effect is quite different from the effect of the excluded volume. Note that for linear chains built from the spherical entities there is an additional factor, influencing the value of the scaling exponent, namely, for spherical droplets/monomers the value of the bond angle is limited to the values of $|\theta| < 120^\circ$. Actually, restrictions imposed on the bond angle reword the “excluded volume restrictions”, and emerge from the fact that droplets do not overlap (see Appendix A).

The restrictions imposed on the bond angle make linear chains less compact and explain satisfactorily the observed value of the exponent ν established for these chains. Consider also that the resemblance of the linear droplet cluster to a free polymer chain should not be exaggerated. Indeed, the linear droplet cluster is not an isolated system; it is embedded into the complicated aerodynamic field. Thus, it is more similar to the polymer chain exerted to the external field. Hence, the value of the scaling exponent ν should be taken *cum grano salis*.

Figure 2 presents the results of measurements of the averaged end-to-end distance labeled \bar{r} normalized by the averaged distance between centers of the adjacent droplets, denoted \bar{l} . The measurements were conducted using 823

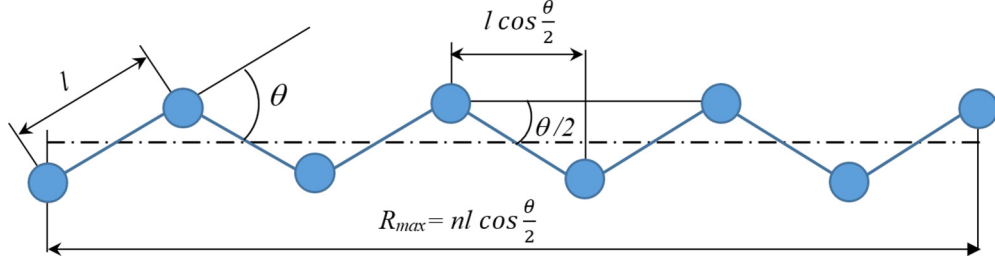


FIG. 3. Schematic of the polymer chain; l is the distance between monomers (droplets); θ is the bond angle, and R_{\max} is the contour length.

nonbranched droplet chains. The linear fitting of the double-logarithmic plot $\log_2 \frac{\bar{r}}{l}$ vs $\log_2 n$, yields the scaling exponent $\nu = 0.76 \pm 0.03$, thus the following scaling law holds:

$$\frac{\bar{r}}{l} = 1.176n^{0.76}, \quad (2)$$

where n is the number of links in the chain or number of bonds. It is recognized from Eq. (2) that the actual value of the scaling exponent is very close to that predicted for 2D models with the excluded volume, rather than to a freely joint-ideal chain [21]. The established scaling exponent $\nu \cong \frac{3}{4}$ corresponds to the value of the excluded volume 2D linear chain in the dilution limit.

Now we address the Kuhn parameters of the 2D chains built of droplets constituting the droplet cluster. The length of the Kuhn segment has to fulfill simultaneously demands imposed by Eqs. (3) and (4), namely,

$$R_{\max} = Nb = nl \cos \frac{\theta}{2}, \quad (3)$$

$$\bar{r} \approx bN^{\frac{3}{4}}, \quad (4)$$

where R_{\max} is the contour length of the chain, and θ is the so-called bond angle (see Fig. 3). It is convenient to introduce the dimensionless values according to: $\tilde{R} = \frac{R_{\max}}{l}$, $\tilde{r} = \frac{\bar{r}}{l}$, and $\tilde{b} = \frac{b}{l}$. Note also that for traditional polymer chains both the bond angle and the distance between molecules is constant, $\theta = \text{const}$; $l = \text{const}$, while for the droplet cluster this is not necessarily true. Droplets forming a pseudopolymer chain do not demonstrate the constant bond angle. The actual distribution of bond angles in the droplet chains is presented in Fig. 4. It is recognized from experimental data shown in Fig. 4 that the distribution of bond angles is not uniform; however $\langle \theta \rangle \cong 0$ takes place; this important observation stems from the spherical symmetry of droplets monomers. The nonuniform distribution of the bond angles does not break the spherical symmetry of droplet-monomer binding along the chain; indeed, such molecules as CH_4 or CCl_4 are spherically symmetrical, however characterized by the exact valence angles.

Therefore, instead of the traditional bond angle the arithmetic averaged value of its absolute value $|\theta|$ was introduced and the bond length l was equal to its arithmetic average value \bar{l} . Note however that \tilde{R} should be calculated with account for the arithmetic average of the cosine (experimental data illustrated with Fig. 4 yielded: $|\overline{|\theta|}| = 22^\circ \pm 0.5^\circ$ ($\cos \frac{|\theta|}{2} = 0.9665 \pm 0.0014$). Thus, assuming $\nu = 0.75$ [see

Eq. (4)], the constituting dimensionless equations defining the pseudo-Kuhn length \tilde{b} and the dimensionless end-to-end distance \tilde{r} are supplied as follows:

$$\tilde{R} = N\tilde{b} = n \left\langle \cos \frac{|\theta|}{2} \right\rangle. \quad (5)$$

$$\tilde{r} = \tilde{b}N^{\frac{3}{4}} \cong 1.176\tilde{b}N^{0.75}. \quad (6)$$

Combining Eqs. (5) and (6) supplied for the dimensionless Kuhn length the estimation $\tilde{b} = \tilde{r}^4 / \tilde{R}_{\max}^3 \cong 2.12 \pm 0.015$ (the standard error is supplied). The dimensionless length \tilde{b} is measured in the units of the averaged distance between the centers of droplets. Thus, the essential correction of the polymer model, describing levitating droplet clusters [16] is attained. The estimation of the length of the Kuhn segment enables the quantitative analysis of the parameters of the branched droplet clusters, such as shown in Figs. 1 and 5. The value of the averaged modulus of the ‘‘bond angle’’ $|\overline{|\theta|}| =$

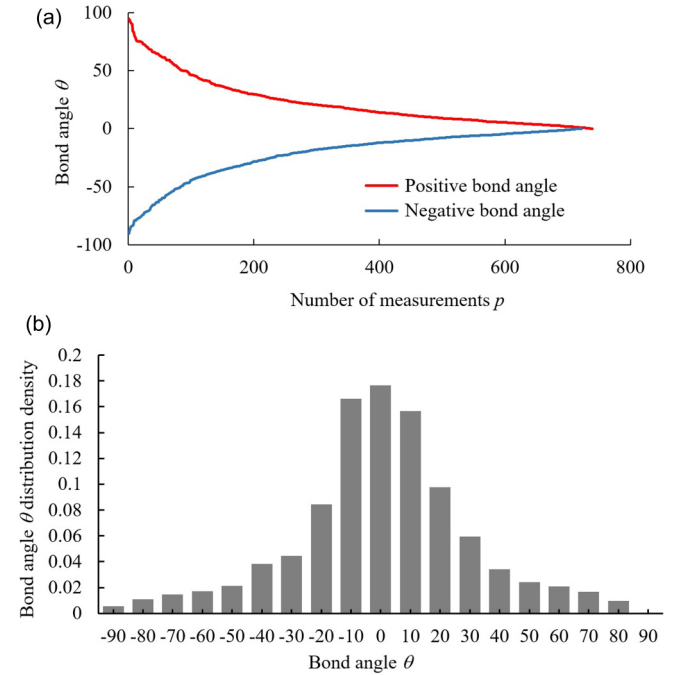


FIG. 4. (a) The distribution of the values of the bond angle θ ; the average absolute values of the bond angle is $|\overline{|\theta|}| = 22^\circ \pm 0.5^\circ$ and $\langle \cos \frac{|\theta|}{2} \rangle = 0.9665$ based on 1443 measurements (734 positive values (red line) and 709 negative values (blue line)). (b) Bond angle θ distribution density is depicted. $\langle \theta \rangle \cong 0$ takes place.

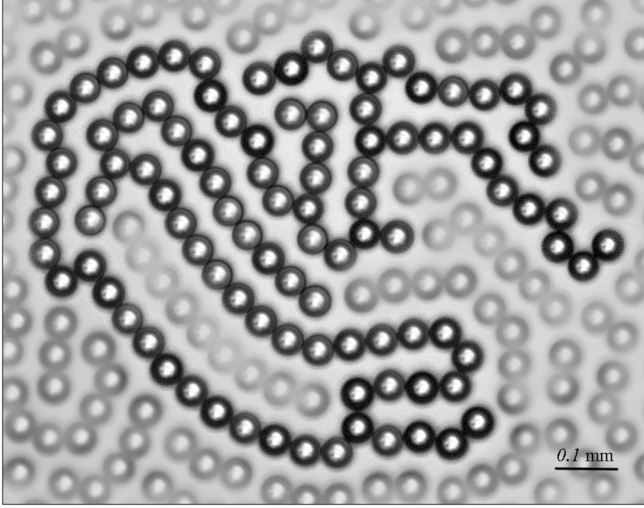


FIG. 5. The branched droplet chain built of 101 droplets (a fragment of cluster 1). The scale bar is 0.1 mm.

$22^\circ \pm 0.5^\circ$ may stem from the peculiarities of aerodynamic interactions responsible for the formation and levitation of droplet chains.

B. Branched droplet clusters and the Kramers theorem

For the branched systems, such as shown in Figs. 1 and 5, the end-to-end distance characterization is not meaningful, and the gyration radius characterizing the system can be introduced

$$R_{g1}^2 = \frac{1}{m^2} \sum_{i=1}^{m-1} \sum_{j=i+1}^m (\vec{R}_i - \vec{R}_j)^2, \quad (7)$$

where m is the number of droplets in the chain.

Alternatively, the square radius of gyration is defined as the average square distance between the monomers and center of mass in a given conformation [21]:

$$R_{g1}^2 = \frac{1}{m} \sum_{i=1}^m (\vec{R}_i - \vec{R}_{cm})^2, \quad (8)$$

where \vec{R}_{cm} is the radius vector of the center of mass of the chain and \vec{R}_i is radius vector of the i th mass. The radius of gyration of a polymer chain about an axis of rotation could be interpreted as the radial distance to a point which would have a moment of inertia the same as the chain's actual distribution of mass, if the total mass of the chain was concentrated. Equation (7) yields the well-known Kramers theorem, enabling a spherical counting method of calculation of the radius of gyration [21]. Let us divide the branched polymer molecule consisting of m monomers with the bond length l into two treelike parts. The first part contains i monomers, and the second part contains $m-i$ monomers correspondingly. The radius of gyration according to the Kramers theorem:

$$R_{g2}^2 = \frac{l^2}{m^2} \sum_{i=1}^{m-1} i(m-i). \quad (9)$$

Introducing the Kuhn segment length b and the number of freely joined effective bonds N enables reformulating of Eq. (9) as follows:

$$R_{g2}^2 = \frac{b^2}{N_m^2} \sum_{N_i=1}^{N_m-1} N_i(N_m - N_i), \quad (10)$$

where $N_m = N + 1$ and N_i correspond to m and i in Eq. (9).

When the radius of gyration is calculated for polymers and other fluctuating objects, the square radius of gyration is usually averaged over the ensemble of allowed conformations giving the mean-square radius of gyration $\langle R_{g2}^2 \rangle$ (see Ref. [25]). For nonfluctuating objects such averaging is not necessary. It is noteworthy that Eq. (9) was derived by Kramers for the ideal freely joint chain [29,30]. However, generalizations of the Kramers theorem exist for the cases when molecular scaling behavior deviates from the classical $1/2$ power exponent of a freely joint chain [31]. It turns out that the Kramers theorem holds for a set of configurations of nonideal chains (see Appendix B and Supplemental Material 2 [25] for examples of gyration radius calculation and generalized Kramers theorem applicability testing.). Thus, the Kramers theorem may be exploited for the estimation of the radius of gyration for nonideal chains. In particular, we checked the validity of the Kramers theorem for the rigid branched chains of droplets, such as depicted in Figs. 1 and 5. To test the Kramers theorem, we calculate the number of freely joined effective bonds N , corresponding to the Kuhn segment b . The Kuhn length of the droplet chain has been established in the previous section. The number N was calculated according to

$$N = \frac{n}{\tilde{b}} \left\langle \cos \frac{|\theta|}{2} \right\rangle, \quad (11)$$

where $\tilde{b} = \frac{b}{l}$ is the dimensionless. The value of N calculated from Eq. (10) was rounded to the nearest integer. When \tilde{b} and N are known, it becomes possible to calculate the radii of gyration using Eqs. (8) and (9) and, therefore, to check the validity of the Kramers theorem for branched droplet chains. It is instructive to introduce the ratio $\frac{R_{g2}}{R_{g1}}$, quantifying the possible deviations from the predictions supplied by the Kramers theorem [in other words, to compare Eq. (8) to Eq. (9)].

We treated the images representing four different droplet branched chains built from the droplets with the average diameter of $5.0 \pm 0.5 \mu\text{m}$. We labeled various branched droplet clusters “1”, “2”, “3” and “4” correspondingly. The results of testing of the Kramers theorem, extracted from the analysis of images of these droplet chains are summarized in Fig. 6. The ratio $\langle \frac{R_{g2}}{R_{g1}} \rangle$ averaged across four clusters was established with the analysis of the images as $\langle \frac{R_{g2}}{R_{g1}} \rangle = 0.91 \pm 0.08$.

For branched chains which do not contain single droplets between branches, we obtained $\langle \frac{R_{g2}}{R_{g1}} \rangle = 0.975 \pm 0.045$, which is in excellent agreement with the predictions of the Kramers theorem. We labeled such droplet chains as the

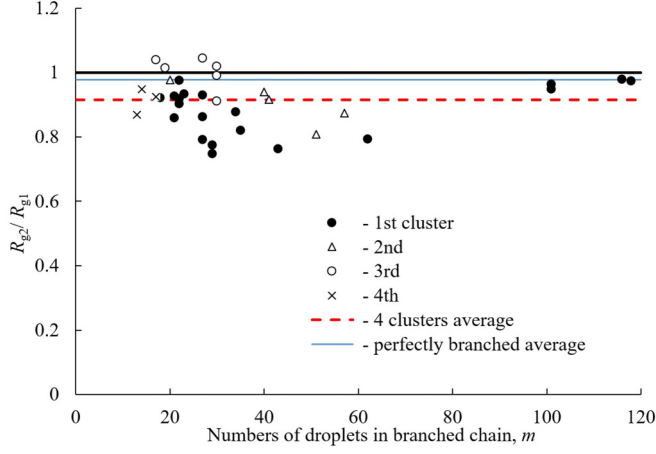


FIG. 6. The ratio $\frac{R_{g2}}{R_{g1}}$ vs the number of droplets calculated for various branched droplet chains for three branched droplet clusters. The dashed line depicts the value of the ratio averaged across four clusters $\langle \frac{R_{g2}}{R_{g1}} \rangle = 0.91 \pm 0.08$ as established for 36 branched chains. Solid blue line depicts the value of the ratio averaged across group of twelve “perfectly branched” chains $\langle \frac{R_{g2}}{R_{g1}} \rangle = 0.975 \pm 0.045$.

“perfectly branched ones”. It is also noteworthy that the Kramers theorem works reasonably well for long ($m \cong 100$) droplet chains. Long chains yielded $\langle \frac{R_{g2}}{R_{g1}} \rangle = 0.965 \pm 0.015$ (See Supplemental Material 2 [25] for detailed analysis).

IV. CONCLUSIONS

Droplet clusters levitating above the locally heated water surface demonstrate polymerlike linear and branched structures, built of droplets [17]. This makes it possible to apply the ideas coming from the polymer science for the phenomenological and scaling analysis of the droplet cluster [21,23]. It should be emphasized that the levitating droplet cluster is a 2D object, thus the dimensionless averaged end-to-end distance of the droplet chain \bar{r} normalized to the averaged distance between centers of the adjacent droplets \bar{l} is expected to scale as $\bar{r} \sim n^{3/4}$, where n is the number of links in the chain. This prediction agrees well with the actual scaling law extracted from the analysis of the nonbranched droplet chains, namely $\bar{r} \sim n^{0.76}$. The analysis of the nonbranched droplet chains enabled calculation of the dimensionless Kuhn length \bar{b} and the averaged absolute value of the bond angle $|\bar{\theta}|$ of the droplet chains, established correspondingly as: $\bar{b} \cong 2.12 \pm 0.015$ and $|\bar{\theta}| = 22.0 \pm 0.5^\circ$. The gyration radius of the branched droplet chains was calculated. The origin of the specific value of the bond angle $|\bar{\theta}|$ calls for additional insights; however, it is reasonable to suggest that it reflects the peculiarities of aerodynamics, governing the formation of the droplet cluster.

The predictions of the Kramers theorem, predicting the gyration radius of the branched polymer chains, were validated for droplet chains, and it was established that it works reasonably for the perfectly branched chains, which do not embrace alien droplets entering their volume and it also works for the long ($n \cong 100$) droplet chains. We conclude that the

notions learned from polymer science are effective for the analysis of both nonbranched and branched droplet chains in levitating droplet clusters.

ACKNOWLEDGMENT

The authors gratefully acknowledge the Russian Science Foundation (Project No. 19-19-00076) for the financial support of this work

APPENDIX A: RESTRICTIONS ON THE BOND ANGLE

In linear droplet chains, restrictions imposed on the bond angle affect scaling of the end-to-end distance of the droplet chain.

The pseudopolymer chain built of three water droplet (or two links) yields for the ideal freely joined chains $\bar{r} = \sqrt{l^2 + l^2 + 2l^2 \langle \cos \theta \rangle} = l \times 2^{1/2}$ (consider $\langle \cos \theta \rangle = 0$). For the bond angle limited to the values of $|\theta| < 120^\circ$ the averaged value $\langle \cos \theta \rangle = 0.4135$. Correspondingly $\bar{r} = l \sqrt{2 + 2 \times 0.4135} \approx 1.6814l \approx l \times 2^{3/4}$ (compare with $2^{3/4} = 1.6818$).

Similar calculations may be carried out for a larger number of droplets. Actually, the scaling exponent $\nu = \frac{3}{4}$ stems from the assumption that droplets do not overlap. The restrictions imposed on the bond angle coincide with the excluded volume hypothesis.

APPENDIX B: GENERALIZATION OF THE KRAMER'S THEOREM FOR NON-IDEAL CHAINS

It is usually accepted that the Kramers theorem works for the ideal free jointed polymer chains, when $\langle r^2 \rangle = Cnl^2$ is adopted. We demonstrate that generalization of the Kramers theorem for nonideal chains becomes possible. Consider the chain built of the segments with the length of l , the number of monomers is m . The bond within the chain is arbitrary. The radius of gyration of the chain R_g is given by Eq. (B1):

$$R_g^2 = \frac{1}{m} \sum_{i=1}^m (\vec{R}_i - \vec{R}_{cm})^2 \quad (\text{B1})$$

where \vec{R}_{cm} is the radius-vector of the center of mass of the chain; \vec{R}_i — i th mass position vector. Equation (B1) is easily transformed into Eq. (B2) (consider $\vec{R}_{cm} = \frac{1}{m} \sum_{i=1}^m \vec{R}_i$) [1]:

$$R_g^2 = \frac{1}{m^2} \sum_{i=1}^{m-1} \sum_{j=i+1}^m (\vec{R}_i - \vec{R}_j)^2, \quad (\text{B2})$$

where $\vec{R}_i - \vec{R}_j = \vec{r}_{ij}$ may be expressed with Eq. (B3):

$$\vec{r}_{ij} = \sum_{k=i}^{j-1} \vec{r}_k, \quad (\text{B3})$$

where \vec{r}_k is the vector connecting the k th and $(k+1)$ th masses, obviously $|\vec{r}_k| = l$ is adopted. Equation (B2) may be

TABLE I. Transposition Procedure.

$\sum_{i=1}^{m-1} \sum_{j=i+1}^m (\vec{R}_i - \vec{R}_j)^2$	$\sum_{i=1}^{m-1} \sum_{j=1}^{m-i} (\vec{R}_j - \vec{R}_{j+i})^2$
$r_{12}r_{13}r_{14}r_{15}r_{16}r_{17}r_{18}r_{19}$	$r_{12} r_{23} r_{34} r_{45} r_{56} r_{67} r_{78} r_{89}$
$r_{23} r_{24} r_{25} r_{26} r_{27} r_{28} r_{29}$	$r_{13} r_{24} r_{35} r_{46} r_{57} r_{68} r_{79}$
$r_{34}r_{35}r_{36}r_{37}r_{38}r_{39}$	$r_{14}r_{25}r_{36}r_{47}r_{58}r_{69}$
$r_{45}r_{46}r_{47}r_{48}r_{49}$	$r_{15}r_{26}r_{37}r_{48}r_{59}$
$r_{56}r_{57}r_{58}r_{59}$	$r_{16}r_{27}r_{38}r_{49}$
$r_{67}r_{68}r_{69}$	$r_{17}r_{28}r_{39}$
$r_{78}r_{79}$	$r_{18}r_{29}$
r_{89}	r_{19}

transformed with the transposition procedure. We illustrate the transposition with the example of the chain built of nine masses in Table I and Fig 7.

As a result Eq. (B4) emerges:

$$\frac{1}{m^2} \sum_{i=1}^{m-1} \sum_{j=i+1}^m (\vec{R}_i - \vec{R}_j)^2 = \frac{1}{m^2} \sum_{i=1}^{m-1} \sum_{j=1}^{m-i} (\vec{R}_j - \vec{R}_{j+i})^2, \quad (\text{B4})$$

Involving Eq. (B3) we transform Eq. (B4) as follows:

$$\begin{aligned} (\vec{R}_j - \vec{R}_{j+i})^2 &= (\vec{r}_{j,j+i})^2 = \left(\sum_{k=j}^{j+i-1} \vec{r}_k \right)^2 \\ &= \sum_{k=j}^{j+i-1} r_k^2 + 2r_k^2 \sum_{k=j}^{j+i-1} \sum_{q=1}^{j+i-1-k} \cos \theta_{k,k+q} \\ &= l^2 \left(i + 2 \sum_{k=j}^{j+i-1} \sum_{q=1}^{j+i-1-k} \cos \theta_{k,k+q} \right), \end{aligned} \quad (\text{B5})$$

where $\theta_{k,k+q}$ – angle between vectors \vec{r}_k and \vec{r}_{k+q} .

Exploiting Eq. (B5) we transform Eq. (B4) as follows:

$$\begin{aligned} \frac{1}{m^2} \sum_{i=1}^{m-1} \sum_{j=1}^{m-i} (\vec{R}_j - \vec{R}_{j+i})^2 \\ = \frac{l^2}{m^2} \sum_{i=1}^{m-1} \sum_{j=1}^{m-i} \left(i + 2 \sum_{k=j}^{j+i-1} \sum_{q=1}^{j+i-1-k} \cos \theta_{k,k+q} \right) \end{aligned}$$

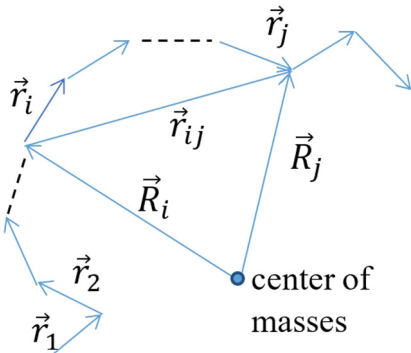


FIG. 7. A polymer chain.

$$\begin{aligned} &= \frac{l^2}{m^2} \sum_{i=1}^{m-1} \left(\sum_{j=1}^{m-i} i + 2 \sum_{j=1}^{m-i} \sum_{k=j}^{j+i-1} \sum_{q=1}^{j+i-1-k} \cos \theta_{k,k+q} \right) \\ &= \frac{l^2}{m^2} \sum_{i=1}^{m-1} i(m-i) + 2 \frac{l^2}{m^2} \sum_{i=1}^{m-1} \sum_{j=1}^{m-i} \sum_{k=j}^{j+i-1} \sum_{q=1}^{j+i-1-k} \cos \theta_{k,k+q}. \end{aligned} \quad (\text{B6})$$

Thus, if Eq. (B7) holds:

$$\sum_{i=1}^{m-1} \sum_{j=1}^{m-i} \sum_{k=j}^{j+i-1} \sum_{q=1}^{j+i-1-k} \cos \theta_{k,k+q} = 0, \quad (\text{B7})$$

we immediately obtain the exact Kramers formula:

$$R_g^2 = \frac{l^2}{m^2} \sum_{i=1}^{m-1} i(m-i). \quad (\text{B8})$$

Recall that m is the total number of monomers within the chain. See numerous examples illustrating Eq. (B7) in the Supplemental Material 2 [25].

Consider that Eq. (B6) was derived for the linear chain. Strictly speaking for the branched chain the value of index i in Eq. (B6) and Eq. (B8) and consequently in Eq. (9) of the main text of the paper is restricted by the lengths of corresponding branches. This problem is usually solved in literature by exact description of the dividing of the branched chain into the subchains, when the sum appearing in Eq. (B8) is calculated. Let us illustrate this with a simple example. Consider linear and branched chains built if four monomers ($m = 4$), depicted in Fig. 4. For the linear chain $i = 1, 2, 3$ when the radius of gyration is calculated. For the branched chain, in which lengths of the branches equal to the single link always $i = 1$.

Let us adjust Eq. (B8) for the branched chain with the single center of branching, depicted in Fig. 8. For a sake of simplicity consider the linear chain as a chain built of two subchains containing n_1 and n_2 links, respectively. Thus, the sum appearing in Eq. (B2) is reshaped as follows:

$$\begin{aligned} &\sum_{i=1}^{m-1} \sum_{j=1}^{m-i} (\vec{R}_j - \vec{R}_{j+i})^2 \\ &= \sum_{i=1}^{n_1} \sum_{j=1}^{n_1-i} (\vec{R}_j - \vec{R}_{j+i})^2 \\ &\quad + \sum_{i=1}^{n_2} \sum_{j=1}^{n_2-i} (\vec{R}_j - \vec{R}_{j+i})^2 + \sum_{j=1}^{n_1} \sum_{i=n_1+1}^{n_1+n_2} (\vec{R}_j - \vec{R}_{j+i})^2. \end{aligned} \quad (\text{B9})$$

Table II presents this dissection amply, using the data, supplied in Table I. As an example for the linear chain built of eight links, vectors \vec{r}_{ij} are bolded for the branches containing $n_1 = 5$ and $n_2 = 3$ links. Vectors connecting monomers in branches with $n_1 = 5$ and $n_2 = 3$ are shown in green and yellow, while purple corresponds to the vectors connecting monomers of the two branches (Supplemental Material 2, Table 6S).

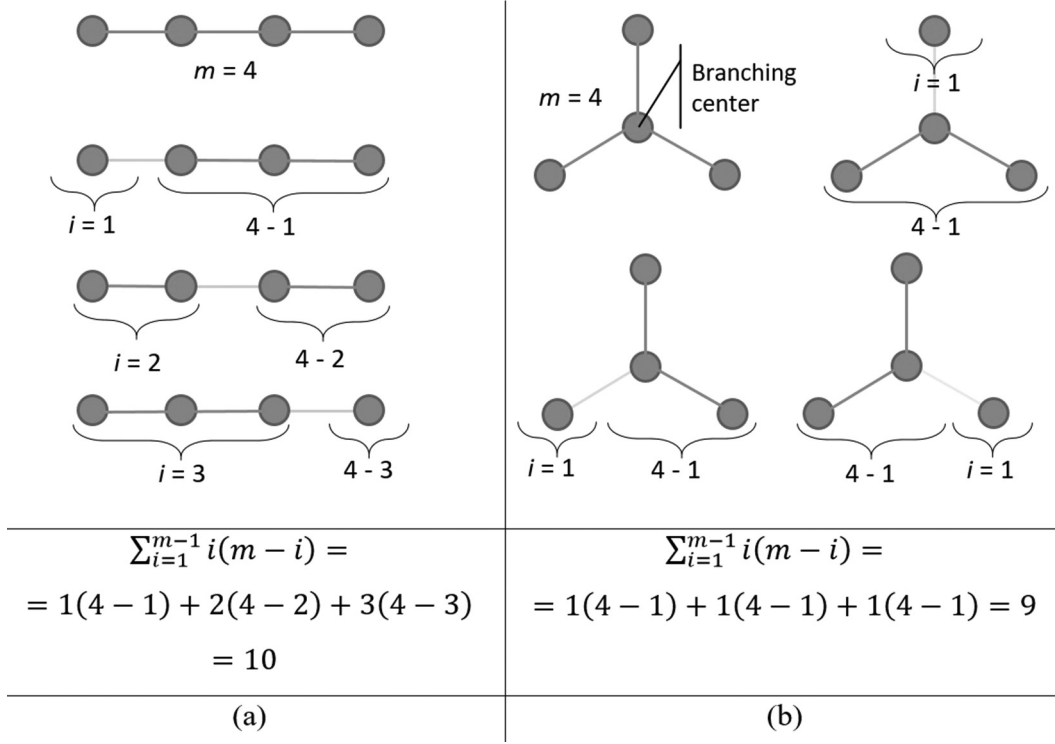


FIG. 8. (a) The linear chain and all of the possibilities of its dividing into two branches are depicted. (b) Branched chain with the single center of branching and various possibilities of its dividing are depicted.

Let us exploit Eq. (B6) and assume the terms containing $\cos \theta$ equal zero. Thus, Eq. (B9) yields

$$R_g^2 = \frac{l^2}{m^2} \left(\sum_{i=1}^{n_1} i(n_1 - i) + \sum_{i=1}^{n_2} i(n_2 - i) + \sum_{j=1}^{n_1} \sum_{i=n_1+1}^{n_1+n_2} i \right). \quad (\text{B10})$$

Taking into account $n_1 = m - n_2 - 1$ and $n_2 = m - n_1 - 1$ enables transformation of the equation appearing in Eq. (B10) as follows:

$$\sum_{i=1}^{m-n_2-1} i(m - n_2 - i) + \sum_{i=1}^{m-n_1-1} i(m - n_1 - i) + \sum_{j=1}^{n_1} \sum_{i=n_1+1}^{n_1+n_2} i$$

TABLE II. The meaning of the vectors appearing in Eq. (B9).

$$\sum_{i=1}^{n_1} \sum_{j=1}^{n_1-i} (\vec{R}_j - \vec{R}_{j+i})^2 + \sum_{i=1}^{n_2} \sum_{j=1}^{n_2-i} (\vec{R}_j - \vec{R}_{j+i})^2 + \sum_{j=1}^{n_1} \sum_{i=n_1+1}^{n_1+n_2} (\vec{R}_j - \vec{R}_{j+i})^2$$

$r_{12} r_{23} r_{34} r_{45} r_{56} r_{67} r_{78} r_{89}$

$r_{13} r_{24} r_{35} r_{46} r_{57} r_{68} r_{79}$

$r_{14} r_{25} r_{36} r_{47} r_{58} r_{69}$

$r_{15} r_{26} r_{37} r_{48} r_{59}$

$r_{16} r_{27} r_{38} r_{49}$

$r_{17} r_{28} r_{39}$

$r_{18} r_{29}$

r_{19}

$$\begin{aligned} &= \sum_{i=1}^{m-n_2-1} i(m-i) - \sum_{i=1}^{m-n_2-1} i n_2 \\ &+ \sum_{i=1}^{m-n_1-1} i(m-i) - \sum_{i=1}^{m-n_1-1} i n_1 + \sum_{j=1}^{n_1} \sum_{i=n_1+1}^{n_1+n_2} i. \end{aligned} \quad (\text{B11})$$

Considering $n_1 + n_2 = m - 1$ gives rise to

$$\begin{aligned} &\sum_{i=1}^{m-n_2-1} i(m-i) + \sum_{i=1}^{m-n_1-1} i(m-i) \\ &= \sum_{i=1}^{n_1} i(m-i) + \sum_{i=1}^{n_2} i(m-i) = \sum_{i=1}^{m-1} i(m-i). \end{aligned} \quad (\text{B12})$$

Consider $\sum_{i=1}^{m-1} i(m-i) \propto R_g^2$. Thus, Eq. (B11) gives rise to

$$\sum_{j=1}^{n_1} \sum_{i=n_1+1}^{n_1+n_2} i - \sum_{i=1}^{m-n_2-1} i n_2 - \sum_{i=1}^{m-n_1-1} i n_1 = 0. \quad (\text{B13})$$

Thus the Kramers formula appears as (again the terms containing $\cos \theta$ are assumed to be equal zero)

$$R_g^2 = \frac{l^2}{m^2} \left(\sum_{i=1}^{n_1} i(m-i) + \sum_{i=1}^{n_2} i(m-i) \right). \tag{B14}$$

Consider now the chain built of three branches; in an analogy to dissection, described by Eq. (B9) we obtain:

$$\begin{aligned} \sum_{i=1}^{m-1} \sum_{j=1}^{m-i} (\bar{R}_j - \bar{R}_{j+i})^2 &= \sum_{i=1}^{n_1} \sum_{j=1}^{n_1-i} (\bar{R}_j - \bar{R}_{j+i})^2 + \sum_{i=1}^{n_2} \sum_{j=1}^{n_2-i} (\bar{R}_j - \bar{R}_{j+i})^2 + \sum_{i=1}^{n_3} \sum_{j=1}^{n_3-i} (\bar{R}_j - \bar{R}_{j+i})^2 \\ &+ \sum_{j=1}^{n_1} \sum_{i=n_1+1}^{n_1+n_2} (\bar{R}_j - \bar{R}_{j+i})^2 + \sum_{j=1}^{n_1} \sum_{i=n_1+1}^{n_1+n_3} (\bar{R}_j - \bar{R}_{j+i})^2 + \sum_{j=1}^{n_2} \sum_{i=n_1+1}^{n_2+n_3} (\bar{R}_j - \bar{R}_{j+i})^2 \end{aligned} \tag{B15}$$

Pairs of indices $n_1 + n_2$, $n_1 + n_3$, $n_2 + n_3$ reflect the fact that in Eq. (B2) we have to account for all of possible combinations of indices i and j . Now it is possible to carry out the dissection similar to Eq. (B9) and Eq. (B15) for the chain built of a branches (a is arbitrary):

$$\sum_{i=1}^{m-1} \sum_{j=1}^{m-i} (\bar{R}_j - \bar{R}_{j+i})^2 = \sum_{b=1}^a \sum_{i=1}^{n_b} \sum_{j=1}^{n_b-i} (\bar{R}_j - \bar{R}_{j+i})^2 + \sum_{b=1}^{a-1} \sum_{c=b+1}^a \sum_{j=1}^{n_b} \sum_{i=n_b+1}^{n_b+n_c} (\bar{R}_j - \bar{R}_{j+i})^2, \tag{B16}$$

where the double sum $\sum_{b=1}^{a-1} \sum_{c=b+1}^a$ represents all of the possible combinations of the pairs of branches. Thus, Eqs. (B14), (B15), and (B16) yield for the chain with a single center of branching the following expression:

$$R_g^2 = \frac{l^2}{m^2} \sum_{b=1}^a \sum_{i=1}^{n_b} i(m-i), \tag{B17}$$

where n_b is the number of chains within the branched labeled by “ b ”. Equation (B17) overcomes the problems inherent for Eq. (B8) (see an example in the Supplemental Material 2).

Considering the terms considering $\cos \theta_{ij}$ yields

$$\begin{aligned} R_g^2 &= \frac{l^2}{m^2} \sum_{b=1}^a \sum_{i=1}^{n_b} i(m-i) \\ &+ 2 \frac{l^2}{m^2} \left(\sum_{b=1}^a \sum_{i=1}^{n_b} \sum_{j=1}^{n_b} \sum_{k=j}^{j-1+i} \sum_{q=1}^{j-1+i-k} \cos \theta_{k,k+q} \right. \\ &\left. + \sum_{b=1}^{a-1} \sum_{c=b+1}^a \sum_{j=1}^{n_b} \sum_{i=n_b+1}^{n_b+n_c} \sum_{k=j}^{j-1+i} \sum_{q=1}^{j-1+i-k} \cos \theta_{k,k+q} \right) \end{aligned} \tag{B18}$$

In the case $a = 2$, Eq. (B17) yields the Kramers formula [i.e., Eq. (B6)] and Eq. (B18) is transformed into Eq. (B8).

Finally interesting to point out that sum in Eq. (B8) can be presented by simple equation:

$$\begin{aligned} \sum_{i=1}^{m-1} i(m-i) &= \sum_{i=1}^{m-1} (im - i^2) = m \sum_{i=1}^{m-1} i \\ &- \sum_{i=1}^{m-1} i^2 = \frac{m(m^2 - 1)}{6}. \end{aligned} \tag{B19}$$

So, for the radius of gyration of a not branched chain we can write the simple formula

$$R_g^2 = \frac{l^2}{6} \frac{(m^2 - 1)}{m}. \tag{B20}$$

[1] G. Forte, R. Burioni, F. Cecconi, and A. Vulpiani, Anomalous diffusion and response in branched systems: A simple analysis, *J. Phys.: Condens. Matter* **25**, 465106 (2013).
 [2] Sh-F. Wang, S. Yang, J. Lee, B. Akgun, D. T. Wu, and M. D. Foster, Anomalous Surface Relaxations of Branched-Polymer Melts, *Phys. Rev. Lett.* **111**, 068303 (2013).
 [3] M. Semsarilar, V. Ladmiral, and S. Perrier, Highly branched and hyperbranched glycopolymers via reversible addition-fragmentation chain transfer polymerization and click chemistry, *Macromolecules* **43**, 1438 (2010).

[4] Ch. Yang and T. Svitkina, Visualizing branched actin filaments in lamellipodia by electron tomography, *Nat. Cell Biol.* **13**, 1012 (2011).
 [5] A. N. Polilov, N. A. Tatus, X. Tian, and A. S. Arutjunova, Equistrong branchy composite beams with a constant total area of variable elliptic cross sections, *Mechanics Composite Mater.* **55**, 325 (2019).
 [6] J. L. Plawsky, Transport in branched systems, *J. Chem. Eng. Communications* **123**, 71 (1993).
 [7] J. P. Richter, *The Notebooks of Leonardo Da Vinci* (Dover, New York, 1970).

- [8] Ch. Eloy, Leonardo's Rule, Self-Similarity, and Wind-Induced Stresses in Trees, *Phys. Rev. Lett.* **107**, 258101 (2011).
- [9] A. Crivoi and F. Duan, Evaporation-induced branched structures from sessile nanofluid droplets, *J. Phys. Chem. C* **117**, 7835 (2013).
- [10] K. Kita, M. Ichikawa, and Y. Kimura, Self-assembly of polymer droplets in a nematic liquid crystal at phase separation, *Phys. Rev. E* **77**, 041702 (2008).
- [11] O. Marin, M. Deutsch, D. Zitoun, and E. Sloutskin, Nanoparticle positioning on liquid and polymerized faceted droplets, *J. Phys. Chem. C* **123**, 28192 (2019).
- [12] R. Tadmor, R. L. Khalfin, and Y. Cohen, Reversible gelation in isotropic solutions of the helical polypeptide poly (γ -benzyl-L-glutamate): Kinetics and formation mechanism of the fibrillar network, *Langmuir* **18**, 7146 (2002).
- [13] Z. Lu, M. H. K. Schaarsberg, X. Zhu, L. Y. Yeo, D. Lohse, and X. Zhang, Universal nanodroplet branches from confining the Ouzo effect, *Proc. Natl Acad. Sci.* **114**, 10332 (2017).
- [14] A. A. Fedorets, Droplet cluster, *JETP Lett.* **79**, 372 (2004).
- [15] A. A. Fedorets, On the mechanism of noncoalescence in a droplet cluster, *JETP Lett.* **81**, 437 (2005).
- [16] A. A. Fedorets, M. Frenkel, E. Shulzinger, L. A. Dombrovsky, E. Bormashenko, and M. Nosonovsky, Self-assembled levitating clusters of water droplets: Pattern-formation and stability, *Sci. Rep.* **7**, 1888 (2017).
- [17] A. A. Fedorets, M. Frenkel, I. Legchenkova, D. V. Shcherbakov, L. A. Dombrovsky, M. Nosonovsky, and E. Bormashenko, Self-arranged levitating droplet clusters: A reversible transition from hexagonal to chain structure, *Langmuir* **35**, 15330 (2019).
- [18] A. V. Shavlov, S. N. Romanyuk, and V. A. Dzhumandzhi, Effective charge and effective radius of water droplet in dropwise cluster, *Phys. Plasmas* **20**, 023703 (2013).
- [19] T. Umeki, M. Ohata, H. Nakanishi, and M. Ichikawa, Dynamics of microdroplets over the surface of hot water, *Sci. Rep.* **5**, 8046 (2015).
- [20] A. A. Fedorets, E. Bormashenko, L. A. Dombrovsky, and M. Nosonovsky, Symmetry of small clusters of levitating water droplets, *Phys. Chem. Chem. Phys.* **22**, 12239 (2020).
- [21] D. V. Zaitsev, D. P. Kirichenko, O. A. Kabov, and V. S. Ajaev, Levitation conditions for condensing droplets over heated liquid surfaces, *Soft Matter* **17**, 4623 (2021).
- [22] V. S. Ajaev, D. V. Zaitsev, and O. A. Kabov, Levitation of evaporating microscale droplets over solid surfaces, *Phys. Rev. Fluids* **6**, 053602 (2021).
- [23] V. S. Ajaev and O. A. Kabov, Levitation and self-organization of droplets, *Ann. Rev. Fluid Mechanics* **53**, 203 (2021).
- [24] A. A. Fedorets, L. A. Dombrovsky, D. N. Gabyshev, E. Bormashenko, and M. Nosonovsky, Effect of external electric field on dynamics of levitating water droplets, *Int. J. Therm. Sci.* **153**, 106375 (2020).
- [25] See Supplemental Material at <http://link.aps.org/supplemental/10.1103/PhysRevE.105.055104> for 1. Video showing dynamic behavior of the chains in the cluster and 2. Examples of gyration radius calculation and generalized Kramers theorem applicability testing.
- [26] M. Rubinstein and R. H. Colby, *Polymer Physics* (Oxford University Press, Oxford, 2003).
- [27] S. Havlin and D. Ben-Avraham, New approach to self-avoiding walks as a critical phenomenon, *J. Phys. A* **15**, L321 (1982).
- [28] P.-G. de Gennes, *Scaling Concepts in Polymer Physics* (Cornell University Press, Ithaca, USA, 1979).
- [29] C. Domb, J. Gillis, and G. Wilmers, On the shape and configuration of polymer molecules, *Proc. Phys. Soc.* **85**, 625 (1965).
- [30] H. A. Kramers, The behavior of macromolecules in inhomogeneous flow, *J. Chem. Phys.* **14**, 415 (1946).
- [31] J. Smrek and A. Y. Grosberg, Understanding the dynamics of rings in the melt in terms of the annealed tree model, *J. Phys.: Condens. Matter* **27**, 064117 (2015).